Spatio-temporal pattern formation with oscillatory chemical reaction and continuous photon flux on a micrometre scale

2005 J. Phys.: Condens. Matter 17 S4239

(http://iopscience.iop.org/0953-8984/17/49/017)

INSTITUTE OF PHYSICS PUBLISHING JOURNAL OF PHYSICS: CONDENSED MATTER

J. Phys.: Condens. Matter **17** (2005) S4239–S4248 doi:10.1088/0953-8984/17/49/017

Spatio-temporal pattern formation with oscillatory chemical reaction and continuous photon flux on a micrometre scale

Hiroyuki Kitahata and Kenichi Yoshikawa[1]

Department of Physics, Graduate School of Science, Kyoto University, Kyoto 606-8502, Japan

E-mail: yoshikaw@scphys.kyoto-u.ac.jp

Received 30 June 2005, in final form 19 July 2005
Published 25 November 2005
Online at stacks.iop.org/JPhysCM/17/S4239

Abstract

Over the past few decades, spontaneous pattern formation in reaction–diffusion systems has been actively studied both theoretically and experimentally. In this article, we report novel phenomena that are generated beyond the framework of usual reaction–diffusion systems: (1) chemical wave propagation under the effect of a boundary, (2) convection in a reaction–diffusion system, and (3) dynamical phase separation under nonequilibrium conditions caused by a focused laser. All of these phenomena are generated as a result of cross-hierarchical interaction between macroscopic and mesoscopic scales.

1. Introduction

To consider how living organisms maintain their lives, it is important to understand the physics in nonlinear open systems, since organisms live through the dissipation of the chemical energy of chemical substances such as adenosine triphosphate (ATP) [1, 2]. Thus, nonlinear open systems have been widely studied from various viewpoints.

In studies on spatio-temporal self-organization caused by chemical reactions, reaction–diffusion systems are used as representative model systems of nonequilibrium open systems. The advantage of a reaction–diffusion system is that spatio-temporal pattern formation can be described using simple equations regarding the dynamics of the local concentrations of the chemicals. Thus, the dynamics of the system can be described as the combination of the local dynamics and transportation from/to the neighbourhood proportional to the gradient, or diffusion.

The diffusion term is derived as follows. Diffusive flow $\vec{J}$ is assumed to be proportional to the gradient of the concentration or some other physical quantity, c,

$$\vec{J} \propto -\vec{\nabla} c. \tag{1}$$

[1] Author to whom any correspondence should be addressed.

From the equation of continuity,

$$\frac{\partial c}{\partial t} = -\vec{\nabla} \cdot \vec{J}, \tag{2}$$

the diffusion equation

$$\frac{\partial c}{\partial t} = D\nabla^2 c \tag{3}$$

is obtained, where D is a positive constant called the 'diffusion constant'.

On the other hand, the dynamics of a chemical reaction can be described using ordinary differential equations based on the mass-action law, which states that the reaction rate is proportional to the product of the concentrations of the reactants.

Taking these two terms into consideration, a reaction–diffusion equation is derived:

$$\frac{\partial c}{\partial t} = f(c) + D\nabla^2 c, \tag{4}$$

where $f(c)$ is the local dynamics of the chemical reaction. For an N-component system, this equation can be easily expanded:

$$\frac{\partial c_i}{\partial t} = f_i(c_1, c_2, \ldots, c_i, \ldots, c_N) + D_i\nabla^2 c_i. \tag{5}$$

Under the framework of such a reaction–diffusion equation, spontaneous pattern formation can be generated theoretically. Turing analyzed spatio-temporal pattern formation, including the generation of travelling waves, in reaction–diffusion systems, and proposed a novel framework of pattern formation called a Turing pattern; i.e., a static pattern can be generated in a two-or-more-component system when the diffusion constants are quite different from each other [3]. It has been reported that the Turing pattern is formed in an actual chemical reaction in a gel [4], and also in the pattern on the skin of a fish [5]. Today, many examples of such pattern formation in living organisms have been found [6]. Moreover, spatio-temporal chaos or chemical turbulence in reaction–diffusion systems has been studied [7].

As an experimental model system, the Belousov–Zhabotinsky (BZ) reaction has been widely adopted [8, 9], since the solution is easily made by mixing four or five chemical reagents and the change is easily observable as a change in colour. Under the proper conditions, the solution of a BZ reaction exhibits oscillation as it is stirred. When the solution is allowed to stand, a spatio-temporal pattern can be observed, such as concentric rings ('target pattern') or expanding spirals ('spiral pattern') as shown in figure 1. These patterns are formed due to the diffusion of the chemical species from the front of the chemical wave. This oscillation and pattern formation can be well reproduced by a numerical model called the Oregonator, which was developed as the adiabatic approximation of the elementary processes in the chemical reaction [10, 11].

Here, it is to be noted that the dynamics of phase separation can also be described by an equation like a reaction–diffusion equation, i.e., the time-dependent Ginzburg–Landau equation and the Cahn–Hilliard equation are often used. These equations are introduced through the variable principle on the total energy of the system. The diffusion-like term $\nabla^2 c$ is derived from the variation of $\int \mathrm{d}\vec{r}|\vec{\nabla}c|^2/2$, where c is an order parameter such as the density or the concentration. Thus, this term reflects the tendency for the system to be uniform. In this sense, this term plays almost the same role as the diffusion term, whereas the derivative of local free energy with respect to the order parameter corresponds to the chemical reaction term in the reaction–diffusion equation.

In this article, we first introduce the experimental results using the BZ reaction, where the behaviours of the reaction–diffusion system are changed due to diffusion near the boundary,

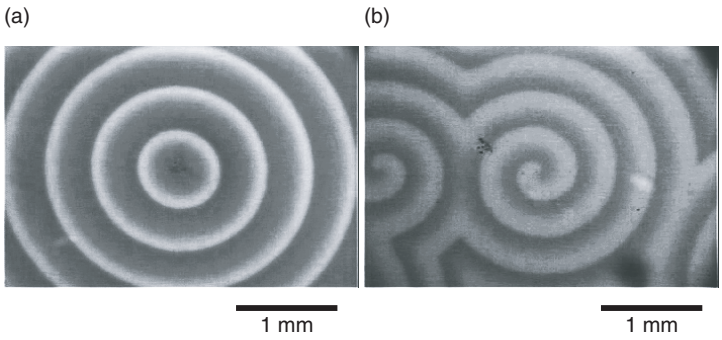

Figure 1. Spatio-temporal patterns in the BZ reaction. (a) A target pattern and (b) a spiral pattern are shown. The brighter and darker regions correspond to the oxidized and reduced states, respectively.

i.e., the behaviours change according to the system size. Next, we describe coupling between convective motion and the reaction–diffusion system. In fact, transport phenomena can be observed in the BZ reaction. Lastly, micrometre-scale phase separation under laser irradiation is introduced. With a change in local conditions, stable phase separation at such a scale becomes possible. By considering these three topics, we will show that diffusion plays an essential role to generate spatio-temporal patterns.

2. Size effect on a reaction–diffusion system

The characteristic distance, $l_{\mathrm{diffusion}}$, that materials are transported by diffusion for a time interval of Δt is

$$l_{\mathrm{diffusion}} \sim \sqrt{D\Delta t}. \tag{6}$$

On the other hand, in the reaction–diffusion system, the chemical wave propagates at a constant velocity, v [12]. The distance, l_{reaction}, that a chemical wave propagates for Δt is

$$l_{\mathrm{reaction}} \sim v\Delta t. \tag{7}$$

Therefore, the diffusion is subjective at a small length-scale, and the propagation of the chemical wave is subjective at a large length-scale. The typical length-scale, l_{c}, at which propagation of the chemical wave is comparable to transport by diffusion is calculated as

$$l_{\mathrm{c}} \sim D/v. \tag{8}$$

The diffusion constant and propagation velocity of the chemical wave are on the order of 10^{-3} and 10^{-2}–10^{-1} mm s^{-1}, respectively. From this estimation, it is expected that

$$l_{\mathrm{c}} \simeq 10^{-2}\text{–}10^{-1}\ \mathrm{mm}. \tag{9}$$

Due to competition between diffusion and chemical wave propagation, an interesting phenomenon can be seen in the BZ reaction on small beads [13], as shown schematically in figure 2. We can observe two different characteristic behaviours of chemical oscillation depending on the size of the beads. On a smaller bead, the diffusion of the chemical reagents predominates, and global oscillation can be seen, i.e., no chemical wave is formed and the whole bead oscillates between the oxidized state and reduced state almost uniformly. On the other hand, propagation of chemical waves can be seen on a larger bead. The critical length is around 100 μm, which almost quantitatively corresponds to the order estimation in equation (9).

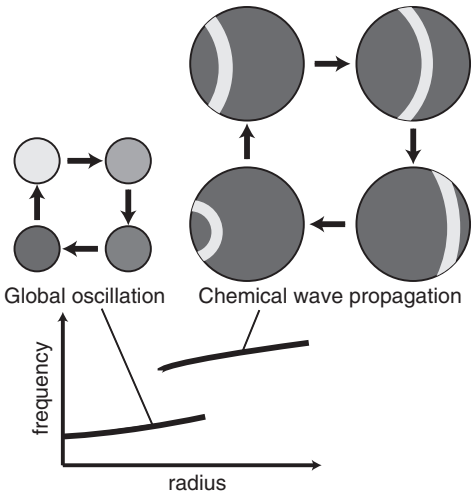

Figure 2. Schematic representation of the characteristics of the BZ reaction on small beads. The BZ reaction exhibits global oscillation on a smaller bead, whereas it exhibits the chemical wave propagation on a larger bead [13].

Another interesting phenomenon using the BZ reaction near the critical length-scale is the propagation failure observed in the BZ medium inside a glass capillary with a decreasing inner diameter [14].

As shown in figure 3, chemical waves were initiated at the wider end by a silver wire without disturbance. A generated chemical wave propagates toward the narrower end, then, slows, stops, and eventually disappears. The oxidized solution in the capillary then reverts to the reduced state. The spatio-temporal plot of images of the capillary along the long axis is shown in figure 3(a), and snapshots at every 5 s are shown in figure 3(b). These clearly show that the velocity of the chemical wave gradually decreases before it stops. This feature was seen in every chemical wave initiated. With each subsequent wave, the position at which the chemical wave stops tends to shift slightly toward the narrower end. This phenomenon can be explained by the effect of the inner surface of the glass capillary, i.e., the diffusion of the chemical reagents changes the velocity of the chemical wave and finally causes propagation failure [14].

It has been shown that the BZ reaction with ruthenium catalyst is light sensitive [15]. In the light-sensitive BZ reaction, a chemical wave cannot propagate in an illuminated area. By taking advantage of this characteristic, we designed the shape of the region in which a chemical wave can propagate. We made a darker area in the shape of a sharp triangle, and the chemical wave propagated from the wider end to the narrower end. The chemical wave stopped propagating as in the glass capillary; however, by controlling the light intensity of the brighter area, the positions at which the chemical wave stopped propagation changed every two waves, as schematically shown in figure 4. It has been suggested that an inhibitor is generated by light illumination [16]. The features of the propagation failure of the chemical waves seem to be affected by diffusion of the inhibitor from the brighter area.

3. Reaction–diffusion system with convection

Under the framework of the reaction–diffusion system, the local concentrations of the chemical reagents have only been described on a fixed field. In the real world, however, convective

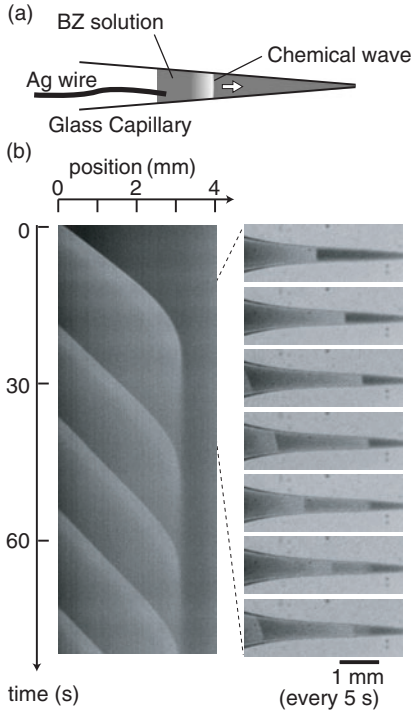

Figure 3. Propagation failure of a chemical wave in the BZ reaction in a glass capillary. (a) Schematic representation of the experimental set-up. (b) Snapshots every 5 s and a spatio-temporal plot made by aligning the lines at the centre of the capillary. The brighter area corresponds to the chemical wave [14].

motion of the field is often observed: for example, as in a chemical reaction in a stirred solution and a biochemical reaction in cytoplasm. To consider this convective motion, an advection term should be added to the reaction–diffusion equation. The flow $\vec{J}$ at the point with a field velocity of v is

$$\vec{J} = -D\vec{\nabla}c + c\vec{v}, \tag{10}$$

instead of equation (1). Based on conservation of the chemical components, the dynamics of c can be written as

$$\frac{\partial c}{\partial t} = D\nabla^2 c - \vec{\nabla}\cdot(c\vec{v}). \tag{11}$$

Here, if the volume of the field is incompressive (for example, the reaction in a solution),

$$\vec{\nabla}\cdot\vec{v} = 0, \tag{12}$$

the advection term can be written as $\vec{v}\cdot\vec{\nabla}c$ instead of $\vec{\nabla}\cdot(c\vec{v})$. Overall, the dynamics of c in the incompressive field can be written

$$\frac{\partial c}{\partial t} = D\nabla^2 c - \vec{v}\cdot\vec{\nabla}c. \tag{13}$$

By adding the local dynamics of the chemical reaction, or the reaction term, reaction–diffusion–advection equations for an N-component system can be written as

$$\frac{\partial c_i}{\partial t} = f_i(c_1, c_2, \ldots, c_i, \ldots, c_N) + D_i\nabla^2 c_i - \vec{v}\cdot\vec{\nabla}c_i. \tag{14}$$

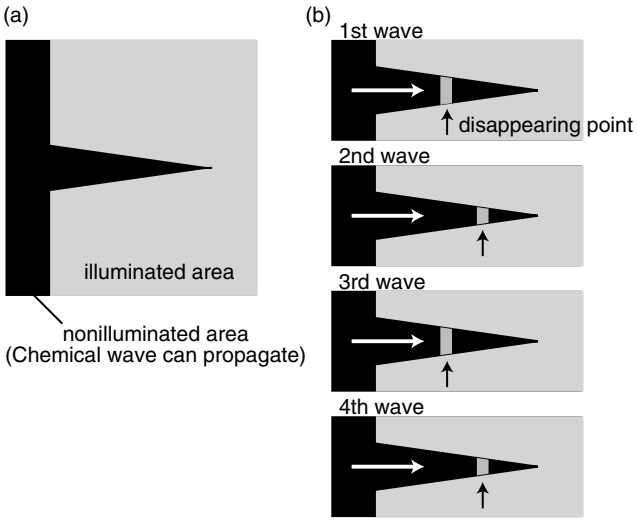

Figure 4. Alternative propagation failure of chemical waves in the light-sensitive BZ reaction system. (a) Schematic representation of the experimental set-up. (b) Schematic illustrations of the experimental results, where the end points of the wave propagation change between near and far positions in a repetitive manner.

We now address convective motion induced by the BZ reaction. The surface tension of BZ medium changes synchronously with the chemical oscillation, and is greater in the oxidized state than in the reduced state [17]. Differences in surface tension induce convective motion called 'Marangoni convection' [18, 19]. It has been shown that convective flow is induced at a gas/BZ medium interface [20], and also at an oil/BZ medium interface [21]. Using this convection, objects are transported along the interface between the BZ medium and oil. An experiment on such unidirectional transport is exemplified in figure 5.

We put some pieces of paper at the interface of the BZ medium and oleic acid, as shown in figure 5(a). The BZ solution is in the excited state, and we put a silver wire into it to initiate a chemical wave. From the point of initiation, chemical waves begin to propagate outward in a concentric manner. The paper moves at the interface toward the wavefront of the chemical wave. Due to the difference in the strength of the convective flow between the regions on both sides of the chemical wave, the paper is transported as shown in figures 5(b) and (c).

This phenomenon is regarded as chemo-mechanical energy transduction, i.e., the chemical energy of the BZ reaction is transduced into the motion of the paper. We have previously demonstrated a system in which chemical energy is transduced into motion under isothermal conditions [22–25]. The theory on chemo-mechanical energy transduction in nonequilibrium open systems has not fully developed in spite of a lot of efforts. We hope the results in the present study may serve as a model experimental system toward the understanding of the essence of the energy transduction.

4. Microscale phase separation under laser irradiation

A focused laser beam can act as optical tweezers, as schematically shown in figure 6, by generating attractive potential due to dielectric interaction [26, 27]. This approach is widely used in various fields such as biology, chemistry, and physics. In general, the optical force can be described in terms of the contribution of two components: the Rayleigh and Mie regimes.

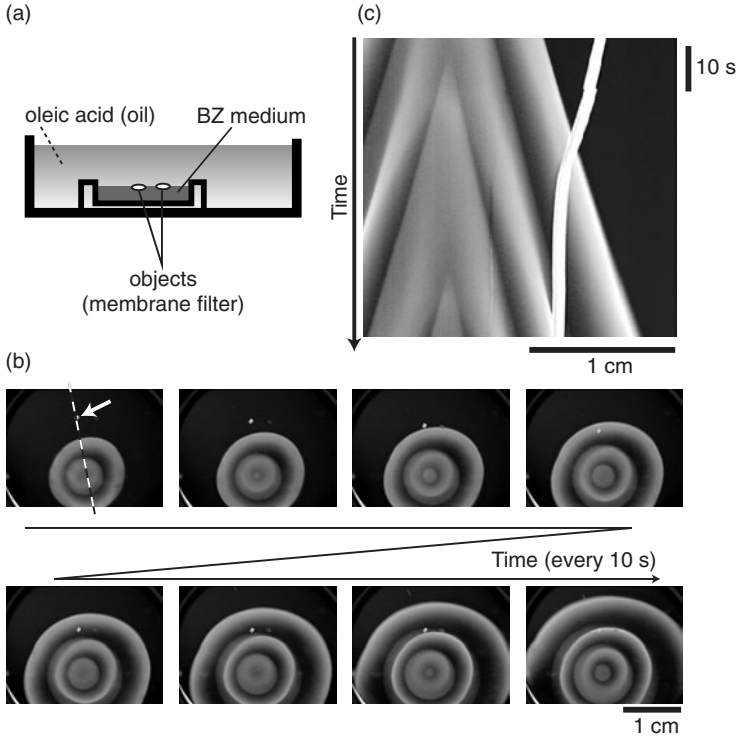

Figure 5. Experiments on the transportation of an object, a piece of paper, at the interface between BZ medium and oil. (a) Schematic representation of the experimental set-up. (b) Snapshots from above every 10 s. The piece of paper shown by the arrow in the first figure was transported by the chemical wave. (c) Spatio-temporal plot made by aligning the pictures on the broken line in the first figure in (b).

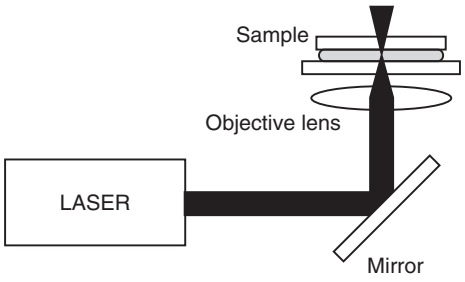

Figure 6. Schematic representation of laser tweezers. The laser beam is focused by an objective lens. Objects or chemical components with a high dielectric constant experience attractive force toward the laser focus.

Since we consider the nucleation of a droplet in this article, we will focus on the Rayleigh regime, where the attractive potential ΔU is given as

$$\Delta U \propto -\langle E^2 \rangle, \tag{15}$$

where $\langle E^2 \rangle$ is the amplitude of the electromagnetic field. This attractive potential can be regarded as the difference in chemical energy. In this section, we show the laser-induced micrometre-scale phase separation due to the attractive force of a focused laser beam.

There have been many studies on phase separation. One of the most popular ways to describe the dynamics of phase separation is the time-dependent Ginzburg–Landau equation and Cahn–Hilliard equation [28].

On a uniform field, a droplet cannot exist stably. The dynamics of the droplet size can be described by the difference in chemical energy between two phases and surface energy. The chemical energy is proportional to the volume of the droplet, and the surface energy is proportional to the surface area. Assuming the droplet has a spherical form with the radius r, the total energy F is

$$F = -\tfrac{4}{3}\pi r^3 \Delta\mu + 4\pi r^2 \gamma. \tag{16}$$

The dynamics of r can be assumed to be proportional to the gradient of the free energy:

$$\frac{\mathrm{d}r}{\mathrm{d}t} = \kappa(4\pi r^2 \Delta\mu - 8\,\pi r \gamma), \tag{17}$$

where κ is a positive constant. From this equation, the critical size of the droplet can be written as

$$r_\mathrm{c} = \frac{2\gamma}{\Delta\mu}. \tag{18}$$

When $r < r_\mathrm{c}$ the droplet shrinks and disappears, and when $r > r_\mathrm{c}$ the droplet becomes larger and larger. From the discussion using the time-dependent Ginzburg–Landau (TDGL) equation for nonconservative systems, the radius of the droplet increases in proportion to the square root of time. Thus, the characteristic size of a droplet is not defined.

In contrast, for conservative systems, the Cahn–Hilliard equation is used. When a droplet is formed, its size increases in proportion to the cube root of time at the initial stage. In an infinite system, the size continues to increase. On the other hand, in a finite system, the final droplet size is determined by the initial components.

This perspective suggests that a small droplet on the scale of a micrometre can hardly exist. On the other hand, under nonuniform conditions, a small droplet can exist. Here, we introduce nonuniformity by irradiation with a continuous laser beam. This laser irradiation can affect the difference in chemical energy, i.e., $\Delta\mu$ in equation (16) should exhibit spatial dependence. The intensity of the laser beam can be written by a Gaussian shape,

$$\langle E^2 \rangle = P \exp\left(-\frac{r^2}{r_0^2}\right), \tag{19}$$

where P is the amplitude of the electromagnetic field at the laser focus. The difference in chemical energy can be written as

$$\Delta\mu = \mu_0 - \mu_1 \langle E^2 \rangle = \mu_0 - \mu_1 P \exp\left(-\frac{r^2}{r_0^2}\right), \tag{20}$$

where μ_0 is the chemical energy difference at the field without laser irradiation. This is because the phase with a higher dielectric constant is more stabilized by laser irradiation, whereas μ_1 is the degree of stabilization by laser irradiation. Using this approach, we can calculate the finite size of the droplet near the laser focus.

In experiments using a water/trimethylamine (oil) system, we observed the gradual development of an oil droplet in the water-rich phase. The oil droplet is trapped at the laser focus. We have also observed some water droplets in the oil-rich phase, which move outward from the focus [29]. The formation of a droplet can be described using Cahn–Hilliard-type equations. We have successfully generated an oil-rich droplet in water-rich solution, and some water-rich droplets in oil-rich solution by numerical calculations; however, these droplets do not move outward. We also observed a nested structure experimentally, where small water-rich

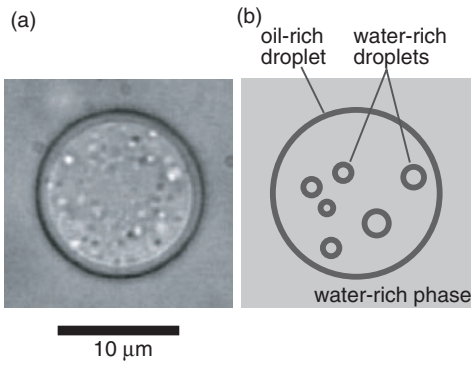

Figure 7. Nested structure: small water-rich droplets in an oil-rich droplet generated in a water-rich phase under laser irradiation. (a) Snapshot of the nested droplets observed by phase-contrast microscopy. (b) Schematic representation of (a).

droplets are generated in a larger oil-rich droplet in a water-rich phase under laser irradiation, as shown in figure 7. We are now considering the mechanism of these dynamical patterns generated under continuous laser irradiation.

5. Summary

To describe nonequilibrium open systems, reaction–diffusion equations can be used. However, for phenomena in the real world, it is not sufficient to consider only the local dynamics (reaction) and diffusion. The present results have shown that the size effect, the convective effect, and local energy injection should be considered. In further studies, it will be important to introduce these optional effects to a reaction–diffusion system in a natural manner.

Acknowledgments

The authors would like to thank Professor J Gorecki (Polish Academy of Sciences, Poland), Dr R Aihara (RIKEN, Japan), Dr T Ichino (Kinki University, Japan) and Dr S Mukai (Japan Agency for Marine-Earth Science and Technology, Japan) for their helpful discussions. This work was supported by Grants-in-Aid for the 21st century COE 'Center for Diversity and Universality in Physics' and for scientific research in priority areas from the Ministry of Education, Culture, Sports, Science, and Technology of Japan.

References

[1] Schrödinger E 1944 *What is Life?* (Cambridge: Cambridge University Press)
[2] Nicolis G and Prigogine I 1977 *Self-organization in Nonequilibrium Systems* (New York: Wiley)
[3] Turing A M 1952 *Phil. Trans. R. Soc.* B **237** 37
[4] Ouyang Q and Swinney H L 1991 *Nature* **352** 610
[5] Kondo S and Arai R 1995 *Nature* **376** 765
[6] Meinhardt H 2004 *Physica* D **199** 264
[7] Kuramoto Y 1984 *Chemical Oscillations, Waves, and Turbulence* (Berlin: Springer)
[8] Zaikin A N and Zhabotinsky A M 1970 *Nature* **225** 535
[9] Kapral R and Showalter K 1995 *Chemical Waves and Patterns* (Dordrecht: Kluwer–Academic)
[10] Field R J and Noyes R M 1974 *J. Chem. Phys.* **60** 1877

[11] Keener J P and Tyson J J 1986 *Physica* D **21** 307
[12] Field R J and Burger M 1985 *Oscillations and Traveling Waves in Chemical Systems* (New York: Wiley)
[13] Aihara R and Yoshikawa K 2001 *J. Phys. Chem.* A **105** 8445
[14] Kitahata H, Aihara R, Mori Y and Yoshikawa K 2004 *J. Phys. Chem.* B **108** 18956
[15] Kuhnert L 1986 *Nature* **319** 393
[16] Agladze K, Obata S and Yoshikawa K 1995 *Physica* D **84** 238
[17] Yoshikawa K, Kusumi T, Ukitsu M and Nakata S 1993 *Chem. Phys. Lett.* **211** 211
[18] Scriven L E and Sternling C V 1960 *Nature* **187** 186
[19] Sørensen T S 1979 *Dynamics and Instability of Fluid Interfaces* (Berlin: Springer)
[20] Miike H, Müller S C and Hess B 1988 *Phys. Rev. Lett.* **61** 2109
[21] Kitahata H, Aihara R, Magome N and Yoshikawa K 2002 *J. Chem. Phys.* **116** 5666
[22] Kitahata H and Yoshikawa K 2005 *Physica* D **205** 283
[23] Nakata S, Iguchi Y, Ose S, Kuboyama M, Ishii T and Yoshikawa K 1997 *Langmuir* **13** 4454
[24] Sumino Y, Magome N, Hamada T and Yoshikawa K 2004 *Phys. Rev. Lett.* **94** 068301
[25] Nagai K, Sumino Y, Kitahata H and Yoshikawa K 2005 *Phys. Rev.* E **71** 065301
[26] Ashkin A, Dziedzic J M, Bjorkholm J E and Chu S 1986 *Opt. Lett.* **11** 288
[27] Ashkin A 1992 *Biophys. J.* **61** 569
[28] Cross M C and Hohenberg P C 1993 *Rev. Mod. Phys.* **65** 851
[29] Mukai S, Magome N, Kitahata H and Yoshikawa K 2003 *Appl. Phys. Lett.* **83** 2557